https://doi.org/10.1016/j.energy.2018.06.033

Numerical study on the impact of runner inlet arc angle on the performance of inline cross-flow turbine used in urban water mains

Du Jiyun*, Shen Zhicheng, Yang Hongxing*

Renewable Energy Research Group (RERG), Department of Building Services Engineering, The Hong Kong Polytechnic University, Hong Kong, China

Abstract

The inline cross-flow turbine is a promising and reliable device to harvest hydropower in an urban water supply pipeline for power supply to its water supply monitoring system. However, investigations about the influencing factors on the performance of inline cross-flow turbines are still rare and this paper focuses on the effect of their runner inlet arc angle for improving the device's performance. Firstly, a mathematical design method for the turbine's blocks is developed. With the proposed method, four models with different runner inlet arc angles are developed. The turbine's performance, function of conversion block, flow velocity characteristics, pressure distribution and blades torque output of the models are then analyzed. Results indicate that a smaller runner inlet arc can increase the flow velocity at runner inlet and pressure difference between the upstream and downstream of the runner, resulting in a higher output power but also a higher overall water head reduction through the turbine. Besides, it is found that the runner inlet arc angle has a significant influence on the power output of runner second stage. With the increase of runner inlet arc angle, the torque output at the second stage encounters a gradual decrease. To achieve a good balance between turbine efficiency and water head reduction, the suggested runner inlet arc angle is 105°. Numerical results showed that the model with 105° runner inlet arc angle could produce a maximum power generation efficiency of 42.6% with about 1.6kW power output.

Keywords: Runner inlet arc angle; urban water mains; micro hydropower; inline cross-flow turbine

1. Introduction

In modern water supply industry, the water monitoring system plays an important role in timely detection and early warning of water leakage, so that water waste in supply process could be reduced [1]. Normally, the water monitoring system achieves its function based on a lot of monitoring devices and sensors, such as flow meters and pressure sensors, which are normally powered by traditional chemical batteries that usually have limited lifespan. Once the batteries ran out, the monitoring system would stop functioning, resulting in serious impact on normal water supply and water security [2]. Instead of chemical batteries, it has been an important research topic to search for constant and stable power sources for water monitoring system.

Renewable energies including wind energy and solar energy are likely to be good alternative power resources for water monitoring system [3,4]. However, these energy sources are uncontrollable and not stable enough. Besides, the harvesting devices are usually bulky and need huge space to install [5]. Considering the fact that most water mains are laid underground, these power sources are not optimal for water monitoring system. Usually, water head in the water mains is high to ensure normal water supply throughout the whole urban area. For instance, in Hong Kong, water head inside urban water mains can research 80m to deliver water through the long water pipes and hilly topography constantly. In addition, water flow inside water mains is continuously available. Therefore, it is likely to be a promising way to harvest hydropower from water mains for power supply to water monitoring system.

Some investigations have been done to study the energy potential of hydropower in the infrastructures of urban water industry. McNabola et al. [6] performed a literature review about micro hydropower installations in water industry, the results indicate that there exists significant potential for hydropower harvesting in water infrastructures. Gallagher et al. [7] proposed a method for site selection and technical assessment of micro hydropower generation in water and wastewater infrastructure. Araya et al. [8]

developed a design method for desalinated water distribution networks which includes energy recovery devices for hydropower generation. These researches not only demonstrate the feasibility of micro hydropower generation from urban mains, but also provide guidance for the application of micro hydropower in water industry.

One of the main challenges for micro hydropower generation in water mains is the selection or design of proper turbines. Generally, micro hydro turbines can be divided into reaction turbines and impulse turbines based on their working principle [9]. The reaction turbines include Francis turbine, propeller turbine and pump as turbine(PAT) while the impulse turbines consist of Pelton, Turgo and cross-flow turbines. Among them, several kinds of turbines have been used for hydropower generation in water supply. A Francis turbine was developed by Tanaka Hydropower Co., LTD in Japan [10] for hydropower generation in water supply pipes. Its maximum installation capacity is 200kW, but its structure is very complex and a huge space is needed for its installation. Lydon et al. [11] conducted three case studies to assess the energy potential in water distribution system using PATs. The results indicate that PAT can convert 40% of the total energy potential of a pressure reducing valve into electricity. Moreover, the PAT also has a good performance in pressure management of the water distribution system. Furthermore, Carravetta et al. [12] developed a PAT installation strategy to keep the backpressure of the PAT stable, hence the PATs can be used to replace pressure reducing valves for hydropower generation as well as water pressure management. However, the literature review about hydropower generation in water pipes using PATs also indicates that water head loss through the PAT is too high at higher flow velocities, so the PAT is not an ideal device for the present research. In addition, several bulb propeller turbines which can be installed inside water pipe were developed [13] [14], but the generator and other electrical components are all submerged in the drinking water, any failure of waterproof may result in severe water pollution.

Compared to other turbines, the cross-flow turbine has a stable efficiency over a wide range of operating flow velocities [15], as the flow velocity inside water mains is

fluctuant due to the variation of user demand over time, the cross-flow turbine seems to be an appreciate device for hydropower generation in urban water mains. In addition, the cross-flow turbine is easy to manufacture and maintain due to its simple structure. There are two main drawbacks for the cross-flow turbine. Firstly, the maximum efficiency of cross-flow turbines is a bit lower than that of other commonly used turbines [15]. Besides, the rotation speed of cross-flow turbines is slow [16]. However, as the power demand and rated voltage of water monitoring meters and sensors are relatively low, the drawbacks of the cross-flow turbines can be neglected.

In our former research, the feasibility of using an inline cross-flow turbine in water supply pipes to harvest hydropower has been studied by numerical and experimental methods [17] [18]. By integrating blocks to the pipe inner wall to function as the nozzle of conventional cross-flow turbines, the inline cross-flow turbine could reach a good performance. In traditional cross-flow turbines, the nozzle shape plays an important role in turbine performance improvement [19] [20]. Similarly, different block shapes have significant impacts on flow velocity and pressure distribution, then further influence the turbine performance. In the proposed inline cross-flow turbine, the block shape is mainly determined by two geometrical parameters: orientation angle of block outlet and the angle of runner inlet arc. Numerical study on the effect of block outlet orientation angle will be presented in a subsequent paper. This paper aims to numerically investigate the influence on inline cross-flow turbine performance caused by runner inlet arc angle.

In the domain of conventional turbine design and optimization, several studies have indicated that the runner inlet arc angle plays a significant role in affecting the turbine performance. Fukutomi et al. [21] studied the influence of nozzle shape upon the turbine performance by theoretical and experimental methods. The results showed that a bigger runner inlet arc angle can lead to a higher value of pressure distribution along the nozzle exit, however, the uniformity of flow attack angle along runner inlet is good for small runner inlet arc angle. The experimental study of Fiuzat and Akerkar [22] indicated that

a cross-flow turbine with 90° runner inlet arc angle has a better performance than that with 120° runner inlet arc angle because more cross-flow exists in the runner of 90° runner inlet arc angle, which leads to a higher efficiency. Besides, the 90°runner inlet arc angle can significantly improve the power output of the runner second stage. A numerical study conducted by Chen et al. [23] showed that the studied cross-flow turbine reaches its maximum efficiency when the runner inlet arc angle is 93°. Currently, the runner inlet arc angle of conventional cross-flow turbine is usually selected as 90° in most of the cases [19] [24] [25]. Many studies have demonstrated that when used in submerged situations, the turbine efficiency is relatively low due to the negative torque on the returning blades caused by water flow. Prasad et al. [26] developed a tidal current turbine by numerical method and the simulation results indicated that the maximum efficiency is recorded 55%. Elbatran et al. [27] designed a cross-flow turbine with dual directed nozzles for application in water channels, the highest efficiency was found 52% when the tip speed ratio (TSR) is 0.5.

As the inline cross-flow turbine used in water supply mains also operates submerged, it is of vital importance to investigate the influencing factors on the performance of cross-flow turbines used submerged and this study mainly focuses on the effect of runner inlet arc angle. Besides, the special application of cross-flow turbine in water supply mains also possesses a higher requirement for water head loss through the turbine as turbine employment cannot have negative impact on normal water supply through the urban area. Therefore, it is necessary to investigate the effect of runner inlet arc angle on water head loss through the turbine. The paper is organized as follows: Section 2 describes the methodologies used in the study, including design method for blocks and runners, numerical method used for turbine performance prediction and flow characteristics analysis, experimental setup and data analysis method. Section 3 presents the main results and analysis, effects of different runner inlet arc angles on the turbine performance and the influencing mechanism is investigated. The main findings are summarized in Conclusion section.

2. Methodology

2.1 Geometrical design

The main parameters for turbine geometrical design are water head and flow velocity in water supply mains. As this paper presents the findings of a research project with the Water Supplies Department (WSD) of Hong Kong, according to the data provided by the WSD, the water head and flow velocity at the design point are 80m and 1.5m/s, respectively. Besides, it is required that water head reduction through the turbine at the design point cannot exceed 5m water.

2.1.1 Block design

The blocks are key components in the proposed inline turbine as they can function as the nozzle in traditional cross-flow turbine. Figure 1 shows the main structure of the inline cross-flow turbine. Two blocks, guide block and conversion block, are integrated to the pipe inner wall. The guide block is used to direct water flow towards the runner while the conversion block can convert part of the water head into flow kinetic energy. Figure 1 also indicates the main geometrical parameters of the blocks and runner. Among them, the orientation angle of guide block θ_0 and runner inlet arc angle λ are two key parameters that determine the shape of conversion block. R_θ represents the distance from runner center axis to the inner wall of conversion block at different azimuthal angles. By determining several R_θ at different azimuthal angles, the geometrical shape of the conversion block can be obtained.

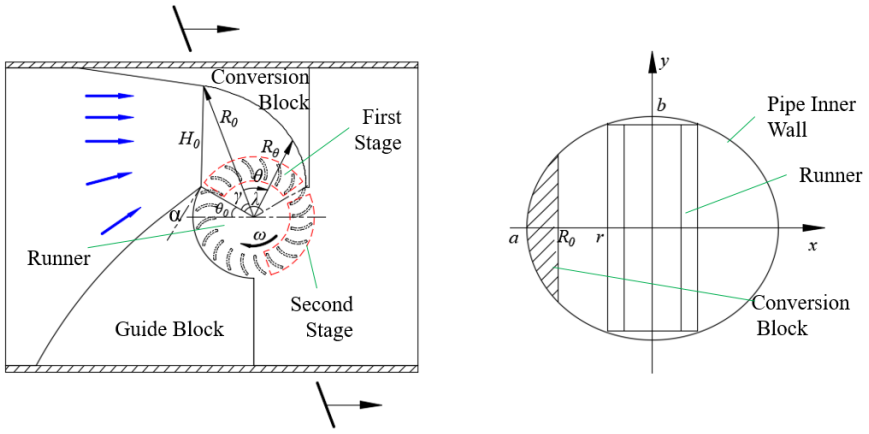

(a) (b)

Fig.1 Design scheme of the inline cross-flow turbine (a) Main structure of the turbine (b) Diagram of cross section at the conversion block inlet

A mathematic design method is proposed for conversion block design, and the design method is developed based on the assumptions that the distribution of water flow rate at the runner inlet arc is uniform and all the reduced water head is converted into flow kinetic energy. The design process can be divided into two steps. The first step is to obtain the distance from runner center axis to the inlet of conversion block, R_0. Based on the first assumption, the flow rate at the inlet of conversion block is:

$$Q_{in} = \frac{\lambda - \gamma}{\lambda} Q \tag{1}$$

where Q is the total flow rate through the runner, m^3/s; λ is runner inlet arc angle; γ is the orientation entry angle of the conversion block.

The orientation entry angle of the conversion block can be calculated by:

$$\gamma = \csc\left(\frac{r\cos\theta_0}{R_0}\right) - \theta_0 \tag{2}$$

According to fluid continuity, the inlet area of the conversion block A_{in} can be calculated:

$$A_{in} = \frac{Q_{in}}{V_{in}} \tag{3}$$

Based on the second assumption and energy equation, the velocity at the block inlet can be determined as:

$$g\Delta H = \frac{1}{2}(V_{in}^2 - V_0^2) \tag{4}$$

where ΔH is the water head reduction through the turbine, m; V_0 is the water flow velocity in the pipe, m/s.

By combining Eq.1-4, the area of conversion block inlet A_{in} can be obtained. Besides that, A_{in} can also be calculated by definite integration. Figure 1(b) shows the cross section of the water pipe through the inlet of the conversion block and runner central axis. The shape of the cross section is an ellipse that can be described as:

$$\frac{x^2}{a^2} + \frac{y^2}{b^2} = 1 \tag{5}$$

$$a = R_{pipe} \Big/ \cos(\frac{\pi}{2} - \theta_0 - \gamma) \tag{6}$$

$$b = R_{pipe} \tag{7}$$

where a is the length of long axes of the ellipse, m; b is the length of short axes of the ellipse, m; R_{pipe} is the inner radius of the water pipe, m; θ_0 is the orientation angle of guide block.

The cross section between the block and runner is a part of the ellipse described by Eq.5-7 and its area $A_{in}^{'}$ can be calculated as:

$$A_{in}^{'} = 2\int_r^{R_0} y dx \tag{8}$$

The definite integral can be solved by substitution method:

$$A_{in}^{'} = \frac{ab}{2}(\sin 2t_2 - \sin 2t_1) - ab(t_2 - t_1) \tag{9}$$

$$t_1 = \csc\frac{r}{a} \tag{10}$$

$$t_2 = \csc\frac{R_0}{a} \tag{11}$$

where, t_1 and t_2 are the substitution parameters; r is the outer radius of the runner, m.

By combining Eq. 2 and 5-11, a calculation method related to R_0 can be obtained for determination of the area of conversion block inlet. It is very difficult to get analytic solution of R_0 but an approximate solution can be acquired based on iteration method. By giving an initial value and a range of R_0, the value of $A_{in}^{'}$ can be calculated. If the value of $A_{in}^{'}$ satisfies the followed equation, this R_0 can be regarded as the required value.

$$\left| \frac{A_{in}^{'} - A_{in}}{A_{in}} \right| \le C \tag{12}$$

where, C is the allowable deviation, 2% is selected in this study.

The second step is to determines the interval values of R_θ at different azimuthal angles, similarly, the flow rate at the cross section through runner central axis and R_θ can be calculated as

$$Q_\theta = \frac{\lambda - \gamma - \theta}{\lambda} Q \tag{13}$$

It is assumed that the flow velocity in the space between the conversion block and runner is uniform, so the area of the cross section through runner central axis and R_θ can be calculated:

$$A_\theta = \frac{Q_\theta}{V_{in}} \tag{14}$$

The elliptic equation of the cross section can be described as:

$$\frac{x^2}{a^2} + \frac{y^2}{b^2} = 1 \tag{15}$$

$$a = R_{pipe} \Big/ \cos(\frac{\pi}{2} - \theta_0 - \gamma - \theta) \tag{16}$$

$$b = R_{pipe} \tag{17}$$

By repeating Eq. 8-12 and using iteration method, the values of R_θ can be obtained and the shape of conversion block can be determined finally.

As the main function of guide block is to direct the water flow to the runner and conversion block. Its main geometrical parameter is the attack angle α which is showed in Figure 1. The attack angle determines the flow inlet direction and its effect on the turbine performance has been studied by several researchers [28] [29] [30]. In this study, the value of attack angle is designed as 22°, which is suggested as the optimum value by the references[24] [30].

2.1.2 Runner design

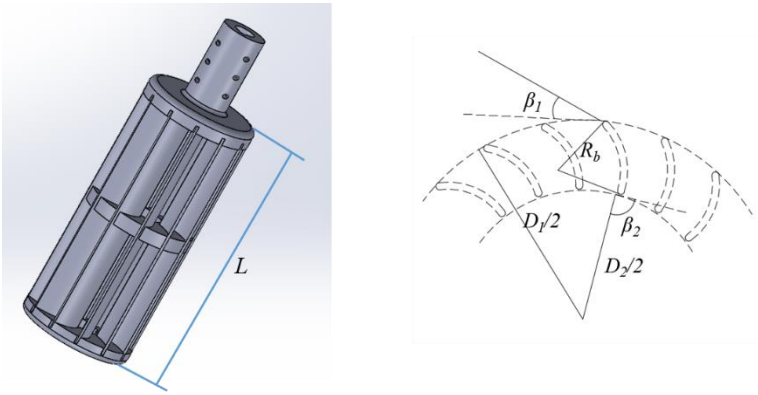

Fig.2 The main geometrical parameters of runner and blades

The runner, which is composed of 20 blades and 3 discs for blades fixing, is the main component for energy harvesting from water flow. The structure and main geometrical parameters of the runner and blades are indicated in Figure 2. The runner's geometrical parameters include the runner length L, outer diameter D_1 and inner diameter D_2 while the geometrical parameters of blades include outer blade angle β_1, inner blade angle β_2 and blade radius R_b. Among them, L is determined by the diameter of water mains, as the runner is inserted in the water mains through a T-joint with diameter of 100mm, D_1 is determined 98mm. Besides, many investigations have demonstrated that β_1, β_2 and the ratio of inner and outer diameter D_2/D_1 have significant effects on cross-flow turbine performance [15] [20], as this paper focuses on the effects of runner inlet arc

220 angle on the turbine performance, β_1, β_2 and D_2/D_1 are determined based on the

221 empirical values suggested in reference [24]. After determination of D_1, D_2/D_1 and

222 β_1, the blade radius R_b can be calculated by:

$$R_b = \frac{D_1^2 - D_2^2}{4D_1 \cos\beta_1} \tag{18}$$

223 Considering the limited space and machining difficulty, the blades number N_b is

224 selected as 20. Table 1 summarizes the values and symbols of runner geometrical

225 parameters.

226 Table 1 The values of runner main geometrical parameters

Geometrical Parameters	Symbols	Values
Blade outer angle	β_1	39°
Blade inner angle	β_2	90°
Outer diameter	D_1	98mm
Inner diameter	D_2	66mm
Ratio of inner and outer diameter	D_2/D_1	0.68
Blade radius	R_b	18.2mm
Blade thickness	T_b	2mm
Blades number	N_b	20
Runner length	L	215mm

227 **2.2 Physical model**

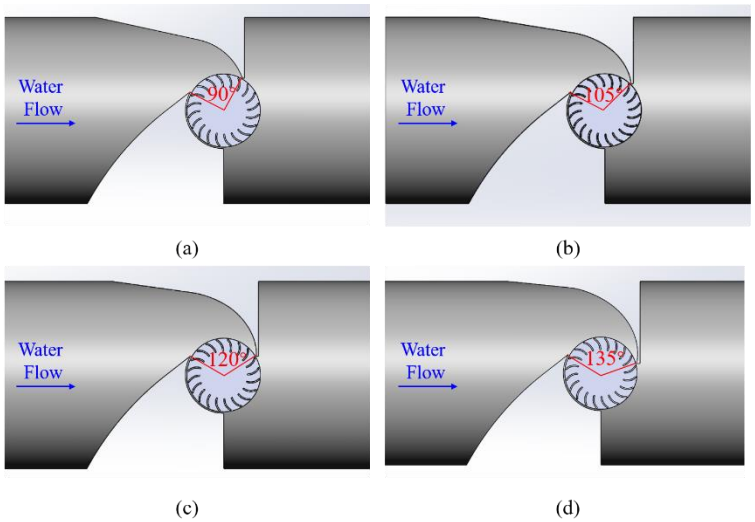

228

Fig.3 Physical models of the inline cross-flow turbine (a) Case 1: λ=90° (b) Case 2: λ=105° (c) Case 3: λ=120° (d) Case 4: λ=135°

To study the impact of different runner inlet arc angles on the turbine performance, four physical models of the inline cross-flow turbine are built using Solidworks 2014 based on the proposed design methods. Figure 3 shows the models studied in this research, the runner inlet arc angles of case 1-4 are 90°, 105°, 120° and 135°, respectively.

2.3 Numerical method

The Computational Fluid Dynamics (CFD) method has been widely used in the domain of flow analysis and performance prediction of hydro turbines [31] [32] [33]. For CFD simulations, computational grids of the physical models (as shown in Figure 4) were generated using ANSYS ICEM 14.5. The whole computational domain is composed of four parts: inlet extension, turbine body, runner and outlet extension. The computational domain was divided into two symmetric parts but only one was modeled and simulated, assuming an impermeable boundary along the symmetry plane. General grid interface is used to connect different parts. These four parts can be divided into two domains: stationary domain which is composed of inlet extension part, turbine body and outlet extension part and the rotating domain consisting of the runner. As the turbine geometry is highly complex due to the curved walls of blocks and narrow tip regions between the runner and blocks, the grids were generated with unstructured tetrahedral mesh. Besides, to increase calculation accuracy, prismatic mesh was adopted for grid generation in the domains near wall boundaries, i.e. the pipe wall and blades. The initial height of prismatic mesh near pipe wall and blades wall are 0.3 and 0.08, respectively, and the number of mesh layers is 10. The average value of y+ near the boundary walls is around 30. In particular, y+ value near the blades wall is around 5. Furthermore, mesh density near interfaces, inlet and outlet is enhanced. To minimize the numerical uncertainty in solution, a grid independence test was conducted considering the output shaft power at the runner rotating speed of 35rad/s. Table 2 shows the shaft power output of four different meshing schemes. According to the results, to achieve a good balance between

calculation time and accuracy, the grid number is selected 3.77 million.

Table 2 Grid independence test results

Grid number (Million)	Shaft power (W)	Variation (%)
1.82	830.9	N/A
2.88	843.5	1.52
3.77	846.3	0.33
5.31	846.6	0.04

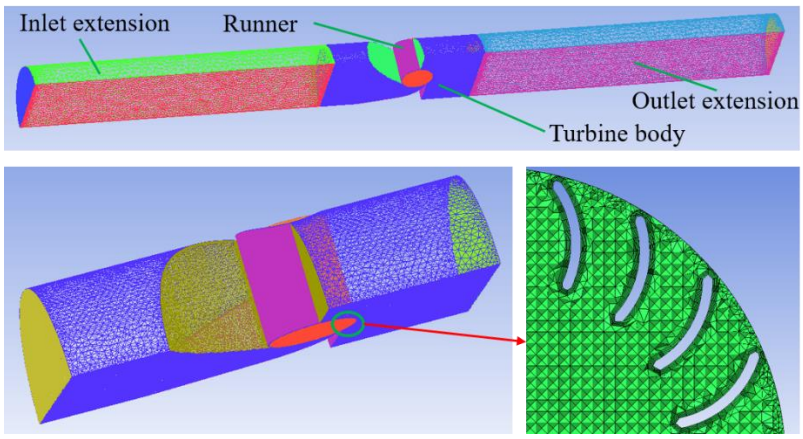

Fig.4 The final meshing scheme of the computational domain

The incompressible isothermal flow through a turbomachine is fully described by the continuity and momentum equations, which are called the Navier-Stokes equations and written as:

$$\frac{\partial u_i}{\partial x_i} = 0 \tag{19}$$

$$\frac{\partial u_i}{\partial t} + u_j \frac{\partial u_i}{\partial x_j} = -\frac{1}{\rho}\frac{\partial p}{\partial x_i} + \nu \frac{\partial^2 u_i}{\partial x_i \partial x_j} \tag{20}$$

where u is the velocity, p is the pressure, ν is the kinematic viscosity of fluid, ρ is the density of fluid.

To solve the Navier-Stokes equations, the Reynolds averaged Navier–Stokes (RANS) method was adopted. RANS equations are obtained by time-averaging the Navier-Stokes equations for the mean values of the flow variables over a sufficiently long period compared to the frequencies of turbulent fluctuations, and are written as:

$$\frac{\partial U_i}{\partial x_i} = 0 \tag{21}$$

$$\frac{\partial U}{\partial t} + U_j \frac{\partial U_i}{\partial x_j} = -\frac{1}{\rho}\frac{\partial P}{\partial x_i} + \frac{\partial}{\partial x_j}\left[v\left(\frac{\partial U_j}{\partial x_i} + \frac{\partial U_i}{\partial x_j} \right) - \overline{u_i' u_j'} \right] \tag{22}$$

where U is the time-averaged velocity, u_i' is the fluctuating velocity due to turbulence and $-\rho\overline{u_i' u_j'}$ is the Reynolds shear stress.

RANS simulations with appropriate turbulence models have been widely used for turbomachinery design analyses due to their low computational cost and satisfactory predictive capability for average device performance [34]. Several turbulence models were proposed to close the RANS equations, e.g. standard $k-\varepsilon$ model, RNG $k-\varepsilon$ model, $k-\omega$ model and SST $k-\omega$ model. Among them, the SST $k-\omega$ model combines the standard $k-\omega$ model and standard $k-\varepsilon$ model, it takes the effects of turbulence shear stress into consideration in the definition of the turbulence viscosity and could capture the micro flow in the viscous layer. Besides, in the reference [15], the author performed CFD simulations with several different turbulence models for performance prediction of cross-flow turbine, the results showed that the SST $k-\omega$ model can be reliable and accurate in numerical study of cross-flow turbines. In this study, the SST $k-\omega$ model is chosen for numerical simulation.

Steady CFD simulations were conducted based on RANS equations with SST $k-\omega$ model using commercial software ANSYS CFX 14.5. In the simulation process, the second-order-accurate finite-volume discretization scheme is selected and the target Root Mean Square (RMS) is set to 10^{-5}. The inlet and outlet boundary conditions are corresponding to the working conditions in the water mains. As the flow velocity and water head are the main parameters for turbine design and the water head on the turbine downstream is an important issue assessing the influence of turbine application on normal water supply, the inlet velocity is considered as the inlet boundary condition of the inlet face while the outlet boundary condition is set as pressure outlet. Besides, the

boundary condition of turbine wall, blocks and blades is set as non-slip smooth wall. For interface, the mesh connection method was automatic.

2.4 Experimental setup and prototype

Fig.5 The preliminary turbine prototype and hydraulic test rig

A hydraulic test rig was built with the help of the WSD and a preliminary turbine prototype was fabricated and tested [18]. As shown in Figure 5 is the turbine prototype and hydraulic test rig. The preliminary prototype was developed in our former research project to study the feasibility of hydropower harvesting from urban water mains. It is mainly composed of a cross-flow runner, a guide block with concave surface and a plate conversion block [18]. The hydraulic test rig was built at Ma On Shan Water Treatment Works (MOSWTW) of Hong Kong. The test rig consists of DN250 pipes, two submersible pumps, the water turbine, an adjustable ball valve and a frequency converter controller. By adjusting the frequency converter controller and the opening degree of ball valve, the flow velocity can be adjusted from 0.5 to 3.0m/s and the maximum water head can reach 80m. For data monitoring and recording, two manometers and an electromagnetic flow meter are used to detect water head and flow velocity, respectively. A 24V three-phase permanent magnet alternating generator with low starting torque is connected to the turbine shaft for electricity generation. A controller was developed for power management and data collection. With the remote communication module of the controller, the monitored water head, flow velocity, turbine rotation speed, charging voltage and current can be recorded in a computer. In

the described test rig, the electromagnetic flow meter has a precision of ±0.5% full scale while the precision of pressure meter is ±0.25% full scale. Using the prescribed methods for uncertainty estimation [35], the composite errors for water head loss and efficiency measurement are ±0.25% and ±0.56%, respectively.

2.5 Data analysis

Tip speed ratio (TSR), which means the ratio of the peripheral speed of the turbine runner and the mean flow velocity at runner inlet and expressed by Equation (23), is an important parameter related to turbine efficiency.

$$TSR = \frac{r\omega}{V} \tag{23}$$

where r is the runner radius (m); V is the mean flow velocity at runner inlet (m/s).

In this research, the flow velocity at runner inlet remains constant. To analyze the effect of TSR on turbine performance, the runner rotation speed was varied in different CFD simulations, so turbine performance under different TSR was obtained.

This study aims to study the effect of different runner inlet arc angle on the performance of inline cross-flow turbine by numerical methods, so it is necessary to validate the accuracy of the numerical results. In the experiments, the turbine performance is assessed based on the power output of generator, however, CFD simulations can only provide the torque output of runner. To compare the experimental and numerical results and to predict the turbine performance more directly, the overall mechanical efficiency and generator conversion efficiency which are determined based on the data provided by parts suppliers are considered. The experimental data are processed using the followed equations:

$$P_{out} = P_{ex} / \eta_{me}\eta_g \tag{24}$$

$$P_{in} = \rho g \Delta H Q \tag{25}$$

$$\eta = \frac{P_{out}}{P_{in}} \tag{26}$$

Where P_{out} is the output power of the shaft, W; P_{ex} is the experimental output power, W; η_{me} is the overall mechanical efficiency; η_g is the conversion efficiency of the generator; P_{in} is the total input power, W; ρ is water density, kg/m^3; g is acceleration of gravity, m/s^2; ΔH is the water head reduction through the turbine, m; Q is the water volume flow rate, m^3/s; η is the turbine efficiency.

3. Results and analysis

In the present paper, a series of CFD simulations were performed to investigate the effects of different runner inlet angles on the inline cross-flow turbine performance. Firstly, the numerical and experimental efficiency of the preliminary prototype are compared for validation. After that, the performance and flow characteristics of turbine models with different runner inlet angles are analyzed.

3.1 Validation of the CFD model

The experimental performance of the preliminary turbine prototype described in part 2.4 at different flow velocities was obtained in the hydraulic test rig. Besides, the physical model of the turbine prototype was built and simulated using the numerical method presented in part 2.3 to study its performance numerically. To compare the numerical and experimental results, the inlet flow velocity and runner rotation speed in simulation process corresponded to that in experimental setup. Figure 6 and Table 3 indicate the comparison between the numerical and experimental turbine efficiency. It can be observed the trend of numerical and experimental efficiency agrees very well, however, there are still some deviations between the experimental and numerical results.

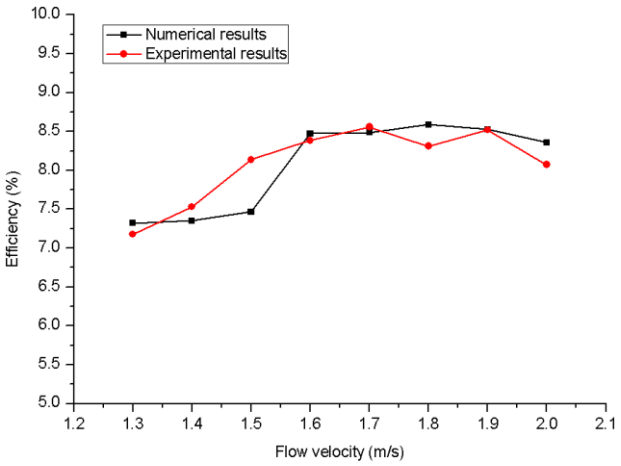

Fig.6 Comparison between numerical and experimental efficiency

Table 3 Numerical and experimental efficiency and relative errors

Flow velocity (m/s)	Experimental efficiency (%)	Numerical efficiency (%)	Error (%)
1.3	7.18	7.32	1.94
1.4	7.53	7.35	-2.39
1.5	8.14	7.46	-8.35
1.6	8.39	8.47	0.95
1.7	8.56	8.49	-0.82
1.8	8.31	8.54	2.77
1.9	8.5	8.53	0.12
2.0	8.07	8.36	3.59

There are two main reasons for the difference between experimental and numerical results. Firstly, the physical models used in CFD simulation is simplified, resulting in calculation uncertainties which are very difficult to be measured and ruled out. On the other hand, the deviations can also be caused by experimental measuring errors. In the test rig, the unstable flow caused by the turbine may result in pressure fluctuation, which has a negative impact on measuring accuracy. However, it can be seen in Table 3 that most of the error percentages in terms of turbine efficiency are limited in ±5%, therefore, the proposed numerical method is suitable for performance analysis of the inline cross-flow turbine regardless of some acceptable errors. In addition, it can also be observed that the efficiency of the developed turbine prototype is relatively low. The main reason for the low efficiency is that the shapes of blocks in the prototype are very

simple and the blocks cannot fully realize their functions. The low experimental efficiency of the proposed turbine prototype also indicates that it is of vital importance to develop a block design method to improve the performance of inline cross-flow turbine.

3.2 Numerical turbine performance

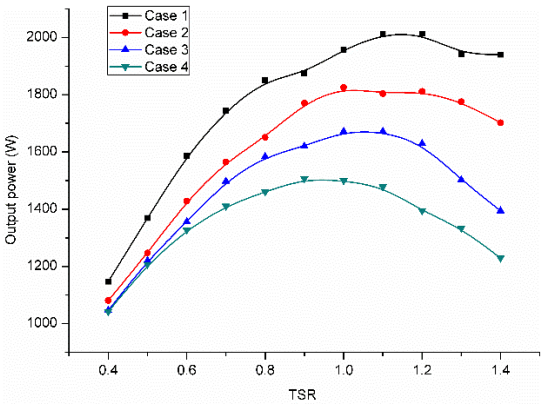

Fig.7 Output power of different cases

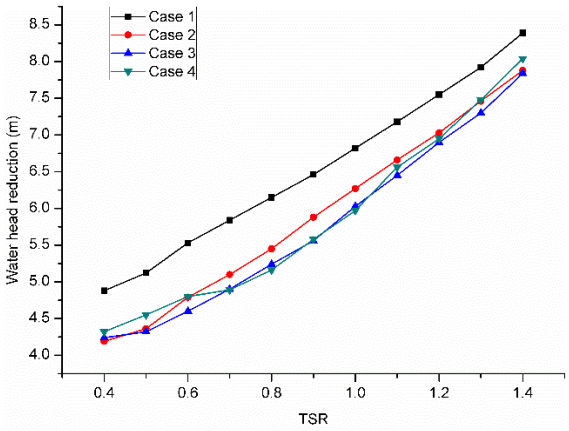

Fig.8 Water head reduction of different cases

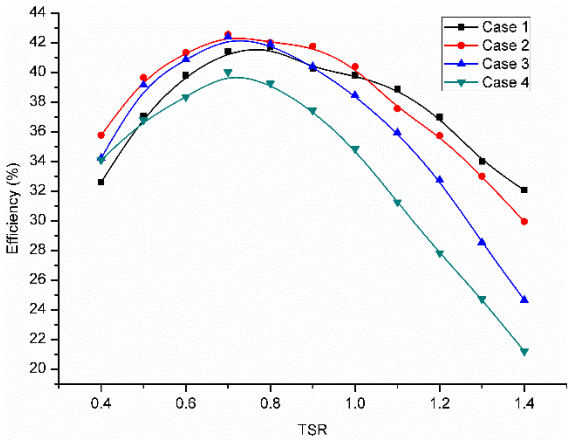

Fig.9 Efficiency of different cases

To fully study effects of different runner inlet arc angle on the inline cross-flow turbine performance, the numerical models of the described cases in Part 2.2 were simulated at different TSRs under the flow velocity of 1.5m/s. Figure 7-9 show the output power, water head reduction through the turbine and efficiency of the four cases, respectively. With the increase of TSR, the output power of four cases increases until reaching maximum, then decrease. By comparing the curves in Figure 7, the turbine output power decreases with the increase of runner inlet arc angle. For example, when λ=90°, the maximum output power is about 1880W, nearly 26% higher than that of the model with λ=135°. Besides, the maximum output power of the four cases occurs when TSR equals to 1.1, 1.0, 1.0 and 0.9, respectively. Figure 8 shows the water head reduction through the turbines with different runner inlet arc angle. The water head reduction of all the four cases increases gradually with the increase of TSR. However, it can be observed that the water head reduction of Case 1 is much higher than that of the other three cases, while Case 2-4 have the similar water head reduction. In term of efficiency, the four cases have the same trend. The maximum efficiency of Case 1 occurs when TSR is 0.8 while case 2-4 get their maximum efficiency at TSR of 0.7. Among the four cases, the overall efficiency of Case 4 is the poorest, only around 39%, for the other cases, the efficiency difference is relatively slight. Case 2 has a better efficiency than the other three models, with the maximum value of 42.6%. It can be concluded that

with the increase of runner inlet arc angle, the best efficiency of inline cross-flow turbine first rises then falls. Besides, Case 2 also keeps a high efficiency in a wide range of TSR. As observed in Figure 8, at the best efficiency TSR, the water head reduction of case 2-4 is around 5m water, which satisfies the requirement of the WSD very well. In conclusion, to achieve a good balance between turbine efficiency and water head reduction, Case 2 is the best model among the four studied cases.

3.3 The function of the conversion block

As described in part 2.1, the main function of conversion block is to convert part of the water head into kinetic energy. To analyze the effect of runner inlet arc angle on the function of conversion block, water head reduction through the conversion blocks of four cases are indicated in Figure 10. In the analysis, the friction and hydraulic loss are ignored, so the reduced water head through the conversion block is converted into kinetic energy completely. As shown in Figure 10, the overall variation trend is that the converted water head rises gradually with the increase of TSR. The case with a smaller runner inlet arc angle can convert more water head. For instance, in Case 1, the conversion block converts 1.35m water head into kinetic energy at TSR of 0.7, while in Case 4, the value is only 0.9m. The variation of converted water head with runner inlet arc angle also provides explanations for the difference of output power and water head reduction in the cases.

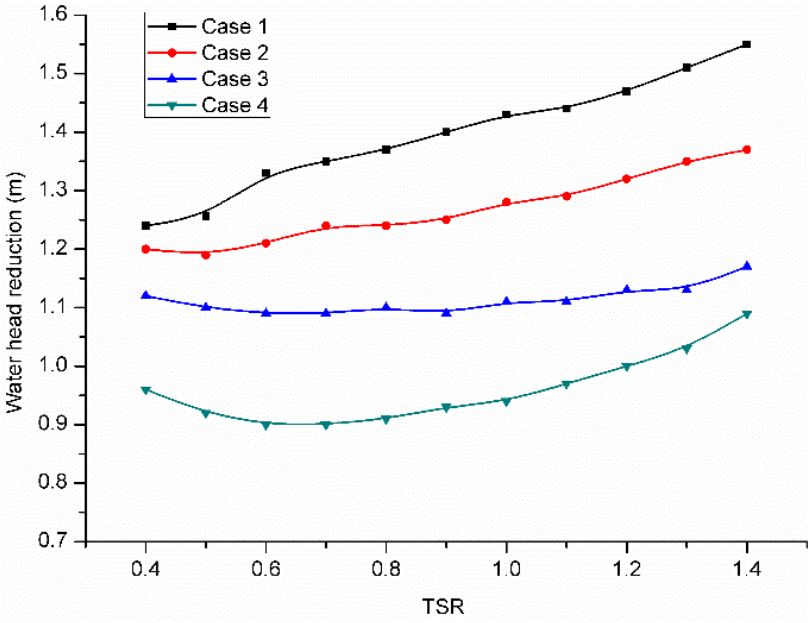

Fig.10 water head reduction through conversion block

3.4 Flow velocity characteristics

The flow velocity characteristics through the proposed inline cross-flow turbine are studied to evaluate the influencing mechanism of runner inlet arc angle on turbine performance. As all the four cases get the best efficiency when TSR equals to 0.7 or 0.8, the flow fields at TSR of 0.7 are analyzed in this research. Figure 11 shows the velocity vectors distribution inside the cross-flow turbine, it can be seen clearly that the proposed blocks have a good function in directing the water flow and enhancing the flow velocity before entering the runner. It can be observed that runner inlet velocity in Case 1 is higher than the other three cases, which means the blocks in Case 1 can convert more water head into kinetic energy. The main feature of cross-flow turbine is that the water flow passes twice through the runner and does work twice on the blades. As shown in Figure 11, the flow velocity in the second stage is higher than that in the first stage as the blades passage in the first stage is converging and the flow velocity is slightly accelerated after leaving the first stage. Comparing the velocity vectors of Case 1-4, in a case with bigger runner inlet arc angle, the water flow passes through more blades, this phenomenon indicates that runner inlet arc angle has an impact on the power

output of each blade and stage and this issue will be discussed in the followed part.

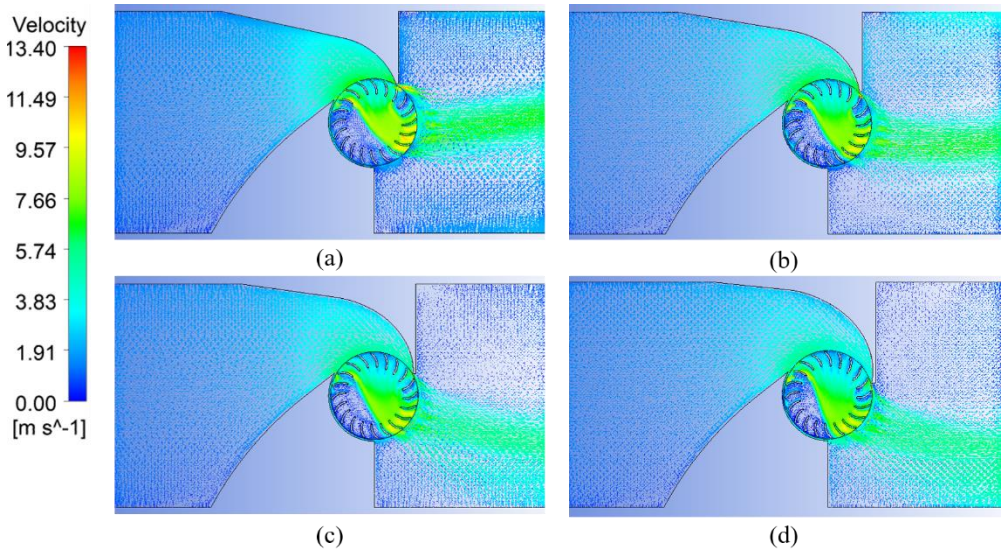

Fig.11 Velocity vectors showing water flow through the inline cross-flow turbine (a) Case 1: λ=90° (b) Case 2: λ=105° (c) Case 3: λ=120° (d) Case 4: λ=135°

Figure 12 indicates the flow velocity distribution along the runner inlet arc of the four cases. To compare the velocities of four cases, the variable of *x* axis in Figure 12 is the position of runner inlet arc. The flow velocity at the runner inlet arc of the cases fluctuates significantly in the range from 4.5-6.5m/s, but it can be observed that the mean velocity reduces slightly with the increase of runner inlet arc angle. After calculation, the mean runner inlet velocity of Case 1-4 is 6.01, 5.79, 5.36 and 5.12 m/s, respectively. The difference between runner inlet velocities also explains why the power output of Case 1 is the highest among four studied cases. As the flow velocity at runner inlet is a crucial factor in affecting the performance of cross-flow turbine, it can be concluded that the runner inlet arc angle plays an important role in influencing the performance of inline cross-flow turbine by determining the runner inlet velocity. It is interesting to note in Figure 12 that the flow velocity at the end of runner inlet arc increases significantly in all the cases. The main reason for this phenomenon is the exist of tip clearance between conversion block and runner and leakage through the tip clearance may accelerate the flow velocity.

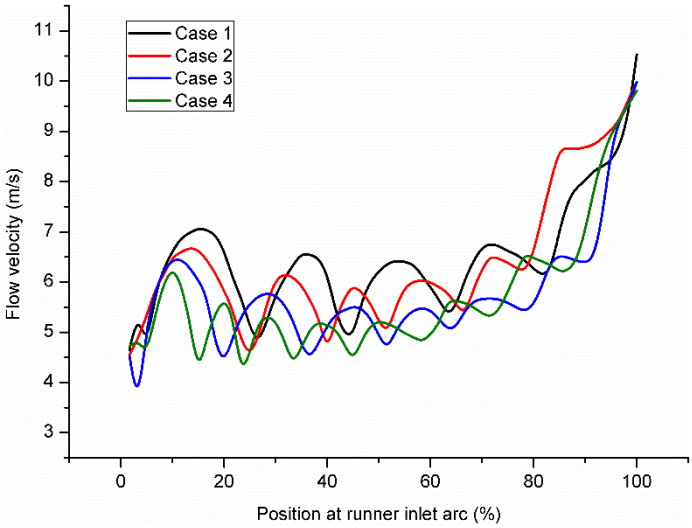

Fig.12 Flow velocity distribution along the runner inlet arc

3.5 Pressure distribution

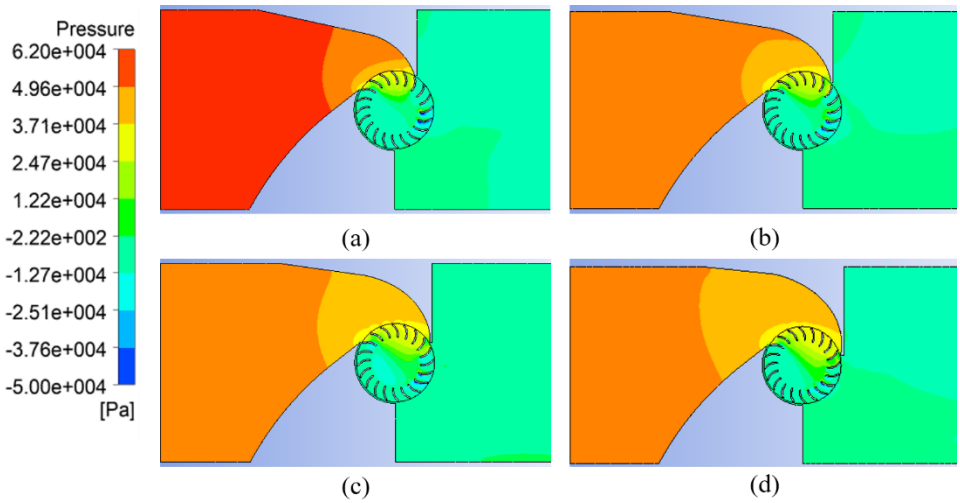

Fig.13 Pressure distribution through the inline cross-flow turbine (a) Case 1: λ=90° (b) Case 2: λ=105° (c) Case 3: λ=120° (d) Case 4: λ=135°

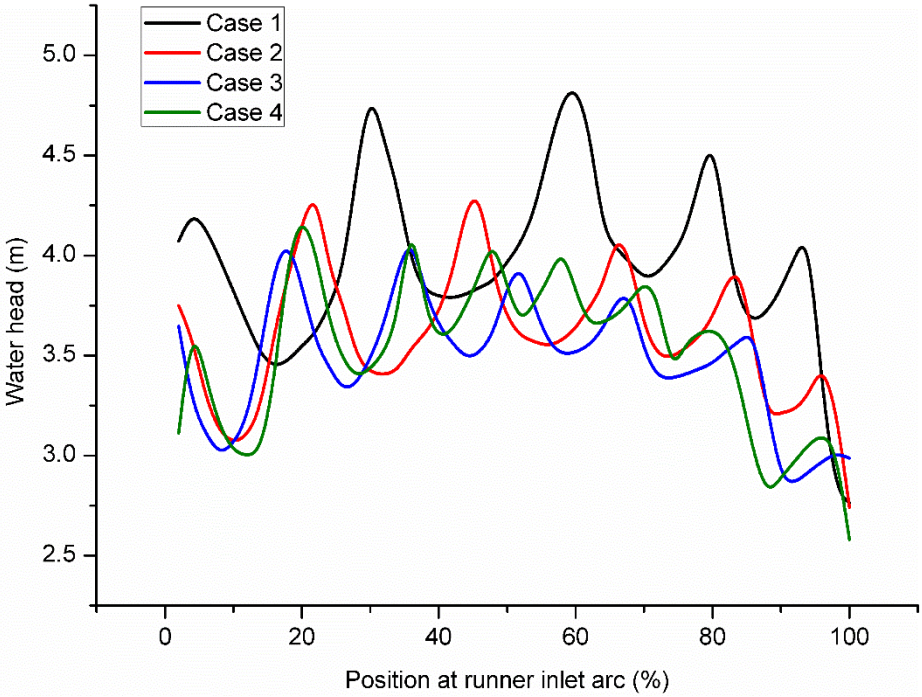

Fig.14 water head distribution along the runner inlet arc

Water head variation in the cross-flow turbine is another factor that influences turbine performance. In this study, the water head distribution through the proposed turbine (as shown in Figure 13) is also investigated. The water head is higher on the upstream side of the runner, then reduces through and behind the runner, where pressure difference occurs. Water head through the conversion block reduces gradually, which is because that the conversion block convert part of the water head into kinetic energy. It can be observed in the blades passages at first and second stage, water head on blade pressure side is higher than that on the suction side, which caused pressure difference. As a result, the force caused pressure difference pushes the blades to rotate from pressure side to suction side thus power is generated. The pressure difference between runner inlet and exit is considered a significant factor in power generation as it can draw in more water and increase the flow velocity [15]. As the downstream water head is considered the same in the four cases, the water head along runner inlet arc is a key factor in output power enhancement of the inline cross-flow turbine. From the pressure contours of the four cases, it is found that the water head at runner inlet reduces slightly with the increase of runner inlet arc angle. Figure 14 compares the actual variation of water head

distribution at runner inlet of all the cases. The water head fluctuates sharply along the runner inlet. It is clear that the average water head at runner inlet of Case 1 is higher than that in the other cases, which corresponds well with the variation showed in Figure 8. In conclusion, a smaller runner inlet arc can increase the pressure difference between the upstream and downstream of the runner, resulting in a higher output power but also a higher overall water head reduction through the turbine.

3.6 Torque of each blade and stage

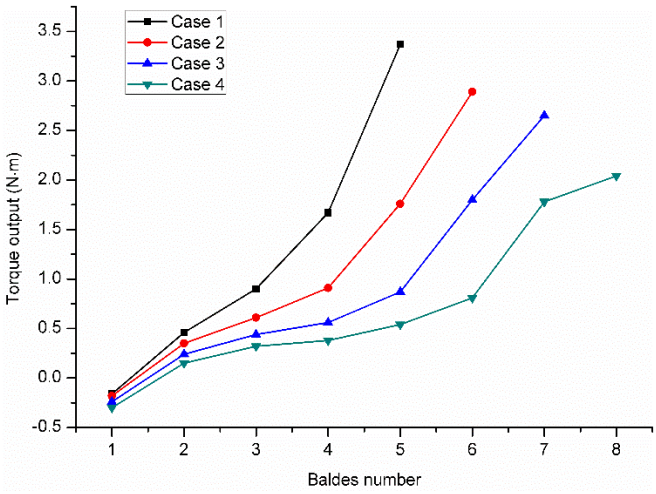

Fig.15 Torque output of each blade at the first stage

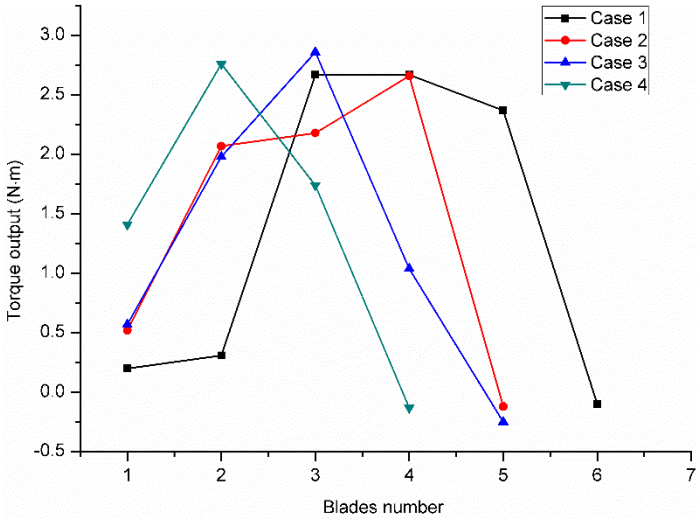

Fig.16 Torque output of each blade at the second stage

To study the effect of runner inlet arc angle on the power of each blade, blades torque

output at the first and second stage is shown in Figure 15 and 16, respectively. Due to the variation of inlet arc angle, the blades number at each stage in different cases is different. As can be seen in Figure 15, although water flow does work on more blades in the cases with bigger runner inlet arc angle, the torque output of each blade is relatively low. The main reason that accounts for this trend is the low flow velocity and water head at runner inlet in these cases. Figure 16 indicates that at the second stage, more blades can generate torque in cases with smaller runner inlet arc angle. Explanation of this phenomenon is that in the cases with a bigger runner inlet arc angle, the exit area of the runner is relatively small, resulting in the number reduction of blades which output torque at the second stage. Figure 17 summarizes the total torque output of the first and second stage. It can be observed that the effect of runner inlet arc angle on the first stage is slight. With the increase of runner inlet arc angle, the torque output at the second stage decreases gradually. For example, the torque output at the second stage in Case 1 is about 40% more than that in Case 4. The main reason for this phenomenon is that in a model with bigger runner inlet arc angle, flow velocity at the inlet of runner second stage is smaller. In addition, it can be seen that in the proposed inline cross-flow turbine, the second stage generates similar or more torque compared to the first stage, this is mainly because of the higher flow velocity through the blades passage at the second stage.

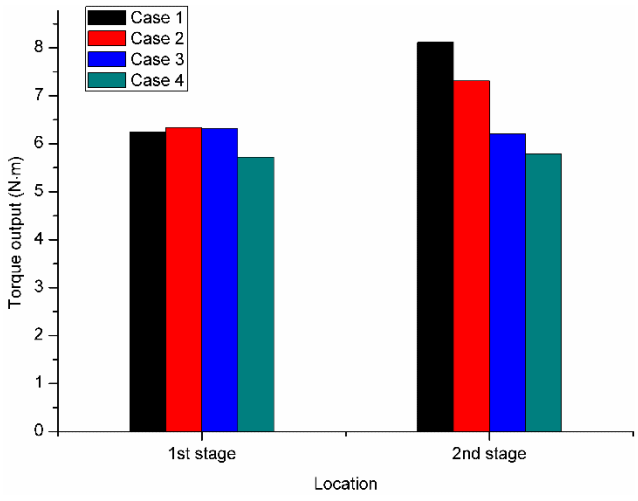

Fig.17 Torque output of each stage

Conclusions

This study aims to investigate the impact of the runner inlet arc angle on the performance of inline cross-flow turbines. Firstly, a mathematic design method for the blocks is developed. With the proposed method, four models with different runner inlet arc angle are built and simulated to obtain an in-depth understanding about the effect and influencing mechanism of runner inlet arc angle on turbine performance. As referred from the present study, the following conclusions can be obtained:

(1) Based on the proposed block design method, the runner inlet arc angle is a key parameter in determining the shape of conversion block. Runner inlet arc angle has an important impact on the function of conversion block. A model with smaller runner inlet arc angle can convert more water head into flow kinetic energy through the conversion block.

(2) A smaller runner inlet arc angle can increase the flow velocity at runner inlet and pressure difference between the upstream and downstream of the runner, resulting in a higher output power but also a higher overall water head reduction through the turbine.

(3) The analysis about torque output of each blade and stage indicates that the runner inlet arc angle only has a slight influence on the power output of runner first stage but has a significant impact on that of runner second stage. With the increase of runner inlet arc angle, the torque output at the second stage encounters a gradual decrease.

(4) To achieve a good balance between turbine efficiency and water head reduction, the suggested runner inlet arc angle is 105°. Numerical results showed that the model with 105° runner inlet arc angle could reach a maximum efficiency of 42.6% with about 1565W power output.

Acknowledgement

The authors would appreciate the financial supports provided by the Innovation and Technology Fund of the Hong Kong Special Administrative Region Government (Grant

542 No.: ITS/032/13) and the help from the Water Supplies Department of the Hong Kong
543 SAR Government.

References

[1] Li W, Ling W, Liu S, et al. Development of systems for detection, early warning, and control of pipeline leakage in drinking water distribution: A case study. Journal of Environmental Sciences, 2011, 23(11): 1816-1822.

[2] Xu Q, Liu R, Chen Q, et al. Review on water leakage control in distribution networks and the associated environmental benefits. Journal of Environmental Sciences, 2014, 26(5): 955-961.

[3] Dondi D, Bertacchini A, Brunelli D, et al. Modeling and optimization of a solar energy harvester system for self-powered wireless sensor networks. IEEE Transactions on Industrial Electronics, 2008, 55(7): 2759-2766.

[4] Weimer M A, Paing T S, Zane R A. Remote area wind energy harvesting for low-power autonomous sensors. system, 2006, 2(1): 2.

[5] Akhtar F, Rehmani M H. Energy replenishment using renewable and traditional energy resources for sustainable wireless sensor networks: A review. Renewable and Sustainable Energy Reviews, 2015, 45: 769-784.

[6] McNabola A, Coughlan P, Corcoran L, et al. Energy recovery in the water industry using micro-hydropower: an opportunity to improve sustainability. Water Policy, 2014, 16(1): 168-183.

[7] Gallagher J, Harris I M, Packwood A J, et al. A strategic assessment of micro-hydropower in the UK and Irish water industry: Identifying technical and economic constraints. Renewable Energy, 2015, 81: 808-815.

[8] Araya N, Cisternas L A, Lucay F, et al. Design of desalinated water distribution networks including energy recovery devices. Computer Aided Chemical Engineering, 2017, 40: 925-930.

[9] Kaunda C S, Kimambo C Z, Nielsen T K. A technical discussion on micro hydropower technology and its turbines. Renewable and Sustainable Energy Reviews, 2014, 35: 445-459.

[10] Tanaka Hydropower Co., Ltd, Products, Available ⟨ http://www.tanakahydro.jp/products/ ⟩ (accessed 11.05.2018).

[11] Lydon T, Coughlan P, McNabola A. Pressure management and energy recovery in water distribution networks: Development of design and selection methodologies using three pump-as-turbine case studies. Renewable Energy, 2017, 114: 1038-1050.

[12] Carravetta A, Del Giudice G, Fecarotta O, et al. Energy production in water distribution networks: A PAT design strategy. Water resources management, 2012, 26(13): 3947-3959.

[13] Saftner D A, Hryciw R D, Green R A, et al. The use of wireless sensors in geotechnical field applications//Proceedings of the 15th annual Great Lakes geotechnical/geoenvironmental conference. 2008.

[14] Ferro L M C, Gato L M C, Falcão A F O. Design of the rotor blades of a mini hydraulic bulb-turbine. Renewable energy, 2011, 36(9): 2395-2403.

[15] Adhikari R. Design Improvement of Crossflow Hydro Turbine. University of Calgary, 2016.

[16] Lahimer A A, Alghoul M A, Sopian K, et al. Research and development aspects of pico-hydro power. Renewable and Sustainable Energy Reviews, 2012, 16(8): 5861-5878.
[17] Chen J, Yang H X, Liu C P, et al. A novel vertical axis water turbine for power generation from water pipelines. Energy, 2013, 54: 184-193.
[18] Jiyun D, Hongxing Y, Zhicheng S, et al. Development of an inline vertical cross-flow turbine for hydropower harvesting in urban water supply pipes. Renewable Energy, 2018, 127: 386-397.
[19] Adhikari R C, Wood D H. A new nozzle design methodology for high efficiency crossflow hydro turbines. Energy for Sustainable Development, 2017, 41: 139-148.
[20] Choi Y D, Lim J I, Kim Y T, et al. Performance and internal flow characteristics of a cross-flow hydro turbine by the shapes of nozzle and runner blade. Journal of Fluid Science and Technology, 2008, 3(3): 398-409.
[21] FUKUTOMI J, NAKASE Y, Watanabe T. A numerical method of free jet from a cross-flow turbine nozzle. Bulletin of JSME, 1985, 28(241): 1436-1440.
[22] Fiuzat A A, Akerkar B P. Power outputs of two stages of cross-flow turbine. Journal of energy engineering, 1991, 117(2): 57-70.
[23] Chen Z, Singh P M, Choi Y D. Effect of Guide Nozzle Shape on the Performance Improvement of a Very Low Head Cross Flow Turbine. The KSFM Journal of Fluid Machinery, 2014, 17(5): 19-26.
[24] Sammartano V, Aricò C, Carravetta A, et al. Banki-Michell optimal design by computational fluid dynamics testing and hydrodynamic analysis. Energies, 2013, 6(5): 2362-2385.
[25] Sammartano V, Morreale G, Sinagra M, et al. Experimental study of cross-flow micro-turbines for aqueduct energy recovery. Procedia Engineering, 2014, 89: 540-547.
[26] Prasad D D, Ahmed M R, Lee Y H. Flow and performance characteristics of a direct drive turbine for wave power generation. Ocean Engineering, 2014, 81: 39-49.
[27] Elbatran A H, Yaakob O B, Ahmed Y M, et al. Novel approach of bidirectional diffuser-augmented channels system for enhancing hydrokinetic power generation in channels. Renewable Energy, 2015, 83: 809-819.
[28] Mockmore C A, Merryfield F. The Banki water turbine. 1949.
[29] Aziz N M, Totapally H G S. Design Parameter refinement for improved Cross-Flow turbine performance. Engineering Report, 1994.
[30] Aziz N M, Desai V R. A laboratory study to improve the efficiency of cross-flow turbines. Engineering Report, 1993.
[31] Du J, Yang H, Shen Z, et al. Micro hydro power generation from water supply system in high rise buildings using pump as turbines. Energy, 2017, 137: 431-440.
[32] Coroneo M, Montante G, Paglianti A, et al. CFD prediction of fluid flow and mixing in stirred tanks: Numerical issues about the RANS simulations. Computers & Chemical Engineering, 2011, 35(10):1959-1968.
[33] Efthimiou G C, Andronopoulos S, Bartzis J G, et al. CFD-RANS prediction of individual exposure from continuous release of hazardous airborne materials in

complex urban environments. 2016:1-23.
[34] Gourdain N. Prediction of the unsteady turbulent flow in an axial compressor stage. Part 1: Comparison of unsteady RANS and LES with experiments. Computers & Fluids, 2015, 106:119-129.
[35] Moffat R J. Describing the uncertainties in experimental results. Experimental thermal and fluid science, 1988, 1(1): 3-17.